Enhancement in Combustion, Performance, and Emission Characteristics of a Diesel Engine Fueled with Ce-ZnO Nanoparticle Additive Added to Soybean Biodiesel Blends

Fayaz Hussain [1], Manzoore Elahi M. Soudagar [2],* , Asif Afzal [3] , M.A. Mujtaba [2] , I.M. Rizwanul Fattah [4],* , Bharat Naik [5], Mohammed Huzaifa Mulla [6], Irfan Anjum Badruddin [7],[8] , T. M. Yunus Khan [7],[8] , Vallapudi Dhana Raju [9], Rakhamaji S. Gavhane [10] and S.M. Ashrafur Rahman [11],*

[1] Modeling Evolutionary Algorithms Simulation and Artificial Intelligence, Faculty of Electrical & Electronics Engineering, Ton Duc Thang University, Ho Chi Minh City, Vietnam; fayaz@tdtu.edu.vn
[2] Department of Mechanical Engineering, Faculty of Engineering, University of Malaya, Kuala Lumpur 50603, Malaysia; m.mujtaba@uet.edu.pk
[3] Department of Mechanical Engineering, P.A. College of Engineering (Affiliated to Visvesvaraya Technological University, Belagavi), Mangaluru 574153, India; asif.afzal86@gmail.com
[4] School of Information, Systems, and Modelling, Faculty of Engineering and I.T., University of Technology Sydney, Ultimo, NSW 2007, Australia
[5] Department of Mechanical Engineering, Jain College of Engineering, Belagavi 590014, India; bharatnaik.bgm@gmail.com
[6] Department of Mechanical Engineering, Jain College of Engineering & Technology Hubballi, Hubli 580032, Karnataka, India; md.huzaifamulla@gmail.com
[7] Research Centre for Advanced Materials Science (RCAMS), King Khalid University, Abha 61413, Asir, Saudi Arabia; magami.irfan@gmail.com (I.A.B.); yunus.tatagar@gmail.com (T.M.Y.K.)
[8] Mechanical Engineering Department, College of Engineering, King Khalid University, Abha 61421, Saudi Arabia
[9] Department of Mechanical Engineering, Lakireddy Bali Reddy College of Engineering, Mylavaram, Andhra Pradesh 521230, India; dhanaraju.v@lbrce.ac.in
[10] Amrutvahini College of Engineering, (Affiliated to Savitribai Phule Pune University, Pune), Sangamner, Ahmednagar 422608, Maharashtra, India; gavhaners@gmail.com
[11] Biofuel Engine Research Facility, Queensland University of Technology, Brisbane, QLD 4000, Australia
* Correspondence: me.soudagar@gmail.com (M.E.M.S.); IslamMdRizwanul.Fattah@uts.edu.au (I.M.R.F.); s2.rahman@qut.edu.au (S.M.A.R.)

Abstract: This study considered the impacts of diesel–soybean biodiesel blends mixed with 3% cerium coated zinc oxide (Ce-ZnO) nanoparticles on the performance, emission, and combustion characteristics of a single cylinder diesel engine. The fuel blends were prepared using 25% soybean biodiesel in diesel (SBME25). Ce-ZnO nanoparticle additives were blended with SBME25 at 25, 50, and 75 ppm using the ultrasonication process with a surfactant (Span 80) at 2 vol.% to enhance the stability of the blend. A variable compression ratio engine operated at a 19.5:1 compression ratio (CR) using these blends resulted in an improvement in overall engine characteristics. With 50 ppm Ce-ZnO nanoparticle additive in SBME25 (SBME25Ce-ZnO50), the brake thermal efficiency (BTE) and heat release rate (HRR) increased by 20.66% and 18.1%, respectively; brake specific fuel consumption (BSFC) by 21.81%; and the CO, smoke, and hydrocarbon (HC) decreased by 30%, 18.7%, and 21.5%, respectively, compared to SBME25 fuel operation. However, the oxides of nitrogen slightly rose for all the nanoparticle added blends. As such, 50 ppm of Ce-ZnO nanoparticle in the blend is a potent choice for the enhancement of engine performance, combustion, and emission characteristics.

1. Introduction

The ever increasing demand for fossil fuels in the transport and industrial segments have led to their rapid exhaustion [1,2].This has also resulted in increased environmental pollution, which has created a severe concern owing to numerous human health issues [3]. This has led to research on potential alternative fuels such as biodiesel. Biodiesel is a promising and eco-friendly fuel that can replace conventional fossil fuels, particularly petroleum-based diesel [4–7]. It is abundantly available and can fulfill the requirement of worldwide increasing energy demands [8–10]. There are several biodiesel feedstocks such as edible and non-edible oils, viz. palm, *Jatropha curcas*, *Calophyllum inophyllum*, *Ceiba pentandra*, waste cooking oils, and animal fats, viz. tallow and lard [11–15]. However, pure biodiesel has certain limitations to be used in compression ignition (CI) engines, such as high density, poor fuel atomization, cold flow properties, piston ring sticking, cold start problem, and a marginal reduction in the economy of the fuel [7,16,17]. These problems can be attenuated by the blending of biodiesel in diesel in a small percentage. However, that could result in a detrimental effect on some emissions, which can be mitigated by adding additives. The addition of additives results in enhanced performance and reduced exhaust emissions of a CI engine [18–21]. Current research focuses on the significance of fuel modification techniques through the use of additives for attaining improved engine performance and reduced emission characteristics.

Nanoparticles used as an additive to the biodiesels have delivered promising results such as improvement in performance and a considerable reduction in the emissions [9,22,23]. Nanoparticle additives (nanoadditives) are mainly known for reducing the emissions of a CI engine [9,24–26]. Nanoadditives lower the CI engine emissions because the metallic particles react with water molecules, creating hydroxyl radical during combustion, which improves complete oxidation of soot particles by reacting with the carbon atom in the soot particles, thus reducing the oxidation temperature [27,28]. Fangsuwannarak et al. [29] concluded titanium oxide nanoparticles with biofuel constantly initiated complete combustion of hydrocarbons resulting in significant reductions in CO, HC, and NOx. Jung et al. [30] reported that use cerium oxide in diesel fuel results in a decrease in combustion lag, which reduces soot formation and complete combustion of fuel take place. Due to this, the combustion rate increases at the current intake. In general, cerium nanoparticles promote complete combustion in the diesel engine, thereby reducing the emissions of CO and HC, as well as lowering the BSFC [31]. This is due to metal base nanoparticles reacting with H_2O and producing hydroxyl radicals, which enhances the soot oxidation reducing the combustion temperature [32]. Sajith et al. [33] experimented with a single cylinder CI engine. They concluded that CeO_2 nanoparticles emulsified at 20 and 80 ppm in Jatropha biodiesel (JME) reduced NOx and HC emissions up to a large extent by 30% and 40%, respectively, irrespective of a moderate rise in BTE by 1.5%. Although research has been done on nanoadditives in biodiesel, experimental evaluations of the performance parameters and pollutant emission on two nanoadditives in biodiesel are very few. To address this gap, this study focused on systematic infusion between two nanomaterials and analyzed its effect on engine emission and performance parameters in a single cylinder CI engine. Alagumalai [34] focused on the combustion of partially premixed charge in CI engine. The authors concluded that lemongrass (*Cymbopogon flexuosus*) oil is self-sufficient with proper combustion without distillation or not required any change in chemical composition. Basha and Anand [35] experimented on a single cylinder CI engine to analyze engine parameters, especially performance and combustion. The values of BTE for JME, JME with 5% water emulsion, and JME with 5% emulsion of water with 100 ppm of CNT were 24.80%, 26.34%, and 28.45%, respectively, and subsequently decreased emissions such as soot and NOx.

The purpose of the current investigation is to analyze the influence of 3% Ce coated ZnO nanoparticles and SBME25-diesel fuel blend at varying loads in a CI engine at a CR of 19.5. In the current study, different dosage levels (25, 50, and 75 ppm) of Ce-ZnO nanoparticles were blended with SBME25 using a surfactant through the ultrasonication process. The loads were varied between 20% and 100%, and the effect of the selected fuel blends on engine performance, emission, and combustion were compared. Noted that the current study focused on improving the performance characteristics of SBME25 blend by adding Ce-ZnO nanoparticle. Diesel fuel was used only as a reference fuel.

2. Materials and Methods

The oil was first heated to 70 °C temperature. Esterification was then carried out with concentrated H_2SO_4 and sodium methoxide in a circulating air oven for 60 min. The transesterification reaction was performed by blending NaOH at 6:1 M and heated at a temperature of 60 °C for 1 h. After that, a magnetic stirrer was utilized to simultaneously mix and heat the mixture for 30 min at 60 °C. The product of this reaction was then moved to a separating funnel for 24 h. Two separate layers of biodiesel and glycerol were seen. The glycerol, which was the lower layer, was removed. The top layer of biodiesel was washed with warm water to obtain pure biodiesel (SBME).

The fatty acid composition of soybean biodiesel (SBME) was estimated using gas chromatography–mass spectrometry (GCMS), Shimadzu, Japan (TQ 8030). Table 1 shows the GCMS analysis results; the free fatty acid (FFA) content for soybean biodiesel was validated from preceding research. The methyl ester was produced utilizing the transesterification of soybean oil [36–38]. Figure 1 illustrates the production of soybean biodiesel using transesterification reaction.

Table 1. FFA content of soybean oil [22].

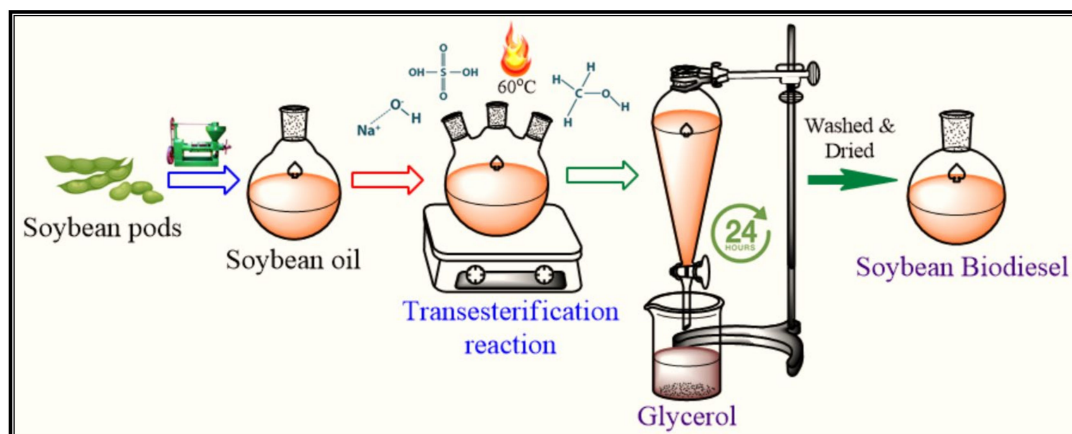| Fatty Acid	Carbon Chain	Composition (wt. %)
Palmitic acid ($C_{16}H_{32}O_2$)	C 16:0	11.24
Stearic acid ($C_{18}H_{36}O_2$)	C 18:0	4.15
Oleic acid ($C_{18}H_{34}O_2$)	C 18:1	23.69
Linoleic acid ($C_{18}H_{32}O_2$)	C 18:2	51.66
Linolenic acid ($C_{18}H_{30}O_2$)	C 18:3	6.89

Figure 1. Production of soybean biodiesel using transesterification reaction.

In the present study, a Kirloskar-make, variable CR (VCR), single cylinder, rated power 3.5 KW, water cooled, CI engine was used. Table 2 shows the VCR engine specifications, and Figure 2 shows the VCR test engine setup. The engine characteristics analyses were conducted at Apex innovation labs, India. For the measurement of emissions, a five-gas analyzer and smoke meter were utilized. A hemispherical combustion chamber (HCC), IT of 23.5 °BTDC, 220 bar injection pressure (IP), and a constant CR of 19.5 were employed. The Exhaust Gas Recirculation (EGR) rate was maintained at 3%

(higher EGR percentage may reduce the pressure and increase smoke) at 27 °C. For comprehensive and reliable engine readings, Enginesoft software was used. In addition, data acquisition and the LabVIEW software (National Instruments, Austin, Texas, USA) was employed as a link among the PC and engine sensors for the measurement of the temperature (T) and load, air, and fuel flow. The HC, NOx, and CO emissions were measured by an AVL 473C exhaust gas analyzer and smoke emissions were measured by using AVL smoke meter. AVL 473C determines the emissions of CO and HC by infrared measurement method (non-dispersive infrared) and NO by electrochemical sensors.

Table 2. Specifications of VCR engine test bed used in the current study.

| Parameter	Specification
Number of strokes	Four
Fuel type	Diesel
Cylinder	Single cylinder, water cooled
Rated power (kW)	3.5 kW at 1500 rpm
Cylinder diameter (mm) × Stroke length (mm)	87.5 mm × 110 mm
CR	19.5
Injection Pressure	220 bar
Injection timing	23.5 °BTDC
Fuel tank	15 L with glass fuel metering column
Piezo sensor	Range 5000 psi, with low noise cable
Temperature sensor	RTD, PT100 and thermocouple type K
Rotameter	Eureka, Engine cooling 40–400 LPH; Calorimeter 25–250 LPH
Temperature sensor	Radix, Type RTD, PT100 and Thermocouple, Type K
Load sensor	Load cell, strain gauge type, range: 0–50 kg
Dynamometer	Type eddy current, water cooled with loading unit
Crank angle sensor	Kubler Germany, Resolution 1 Deg, Speed 5500 RPM with top dead center (TDC) pulse
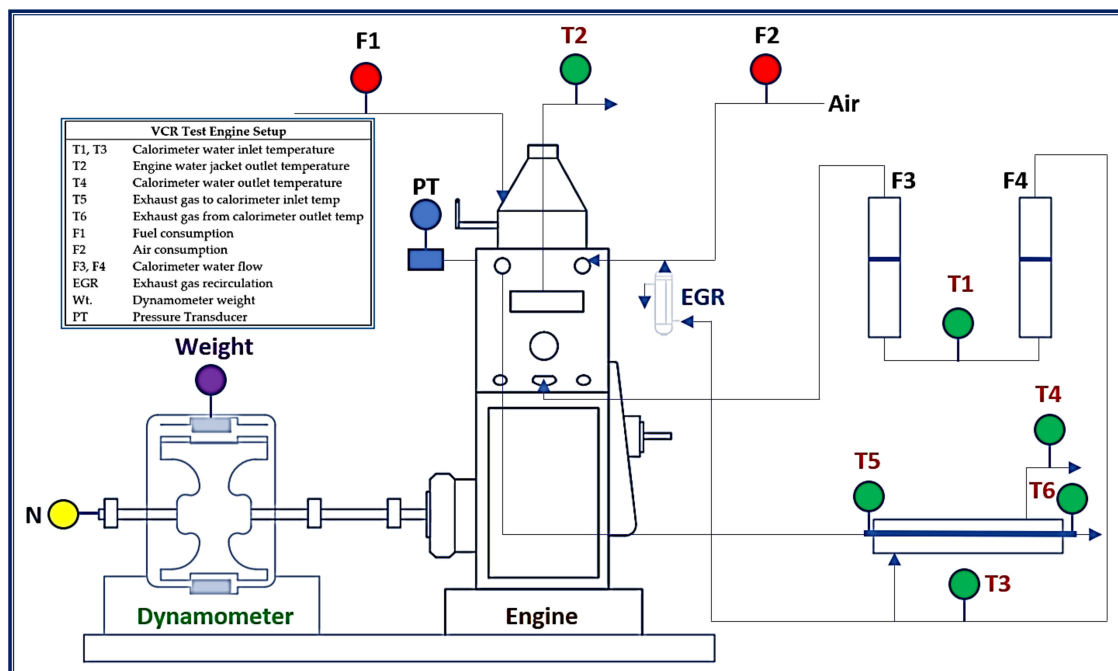
Figure 2. VCR engine test bed setup.

2.1. Production of Ce Doped ZnO Nanoparticle Additives

In a typical synthesis procedure of 3% Ce doped ZnO, zinc acetate dihydrate along with cerium chloride nitrate heptahydrate ($CeCl_3.7H_2O$) with appropriate molar ratio were dissolved in water. Later, 5.027 g disodium succinate hexahydrate was added to the prepared solution, followed by stirring for 20 min using a magnetic stirrer. Then, to the above well-mixed solution, 20 mL of 0.02 M aq. NaOH solution were added dropwise. The resulting mixture was magnetically stirred for 30 min and then transferred to an autoclave of Teflon-lined stainless steel with a capacity of 200 mL, sealed, and held for 20 h at 120 °C. Subsequently, the autoclave automatically cooled to room temperature. The obtained precipitate was centrifuged washed and dried at 50 °C. Figure 3 illustrates synthesis of Ce doped ZnO nanoparticles.
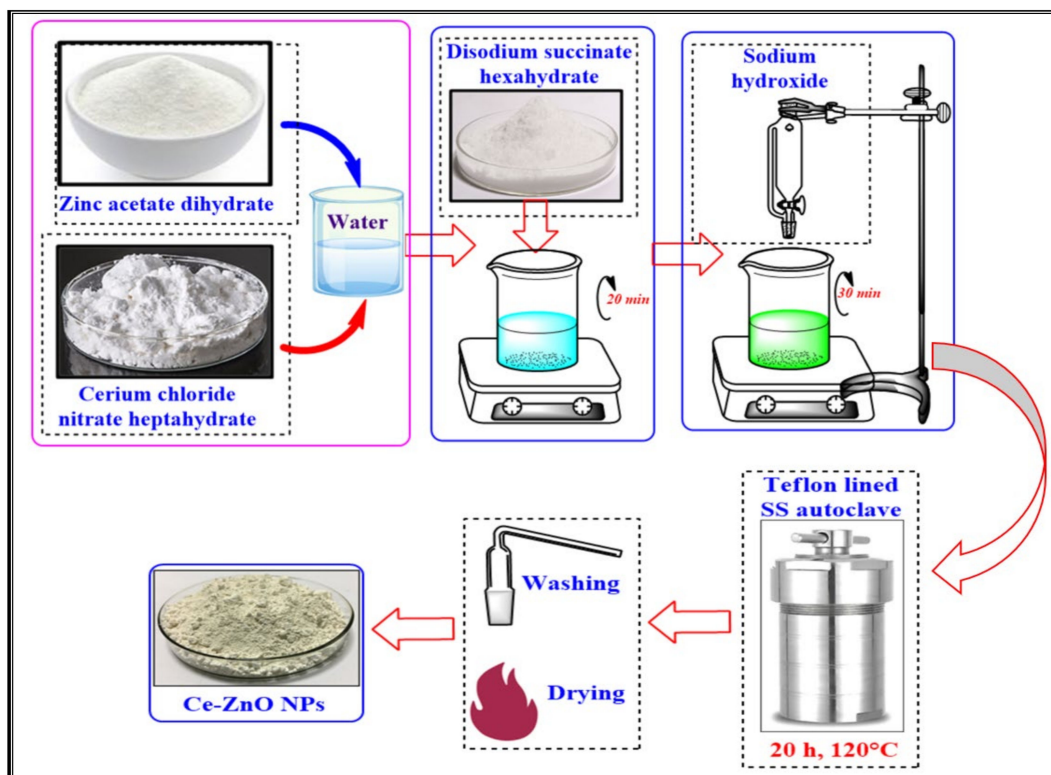

Figure 3. Synthesis of Ce doped ZnO nanoparticles.

2.2. Uncertainty Analysis

The uncertainty analysis is the set of errors obtained during the experimentation process and other external factors. In addition, the uncertainties in the measured values may develop because of errors in the measuring instruments, human errors in measurement of the experimental data and computations errors, and slightly affected by the environmental factors. The ideal conditions are utilized to gather the data. To calculate the uncertainty in the obtained results, the method described by Moffat et al. [39] was used in the current investigation. The propagation of errors was studied by plotting error bars for each reading and taking the average of six experimental readings. Table 3 demonstrates the uncertainty analysis of several parameters.

Table 3. Uncertainty analysis of the obtained results.

Parameters	Accuracy (±)	Uncertainty (%)
BP (kW)	-	±0.5
BTE (%)	-	±0.3
BSFC (%)	-	±0.3
HRR (J/°CA)	-	±0.5
CO emission (%)	±0.01%	±0.3
NOx emission (ppm)	±10 ppm	±0.7
HC emission (ppm)	±10 ppm	±0.4
Exhaust gas temperature (°C)	±1	±0.4
Smoke meter (HSU)	±1	±0.5

2.3. Preparation and Physicochemical Properties of Nanoadditive Fuel Blends

In the current investigation, sorbitan monooleate (Span 80) 2 vol.% surfactant, which is highly dispersible and stable in the base fluid, was blended with 25% diesel–soybean biodiesel blend. For the ultrasonication process, methods discussed in previous studies done by Soudagar et al. [40,41] and Gavhane et al. [22] were used. The blending was carried using the ultrasonication process. Initially, the blend of diesel, span 80, Ce-ZnO nanoparticles (dosage level: 25, 50, and 75 mg/L), and biodiesel was stirred and heated at 60 °C using a magnetic stirrer to remove any water traces followed by bath sonication for an agitation period of 60 min. Figure 4 illustrates preparation of nano fuel blends using ultrasonication.
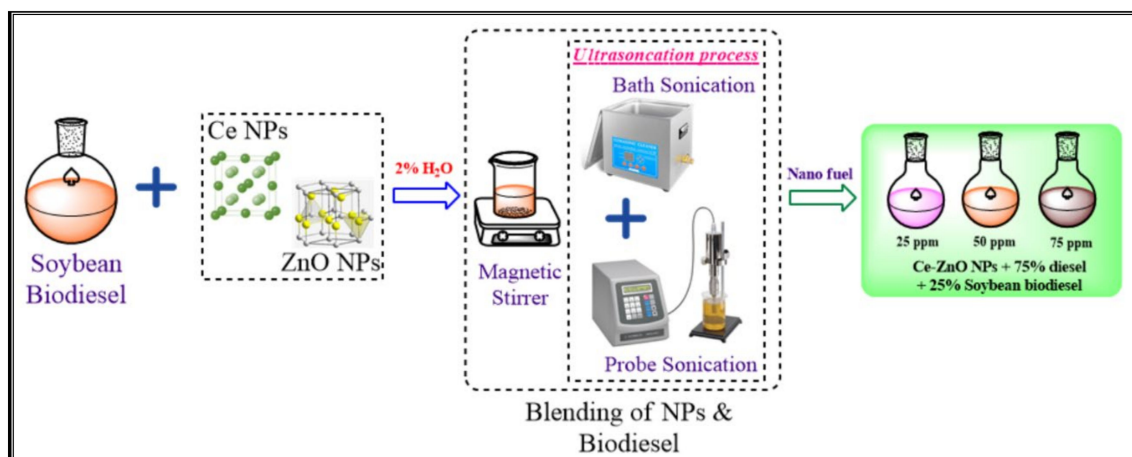

Figure 4. Preparation of nano fuel blends using ultrasonication.

Figure 5 illustrates the schematic representation of probe sonicator. Furthermore, a probe sonicator was used for the sonication process, and the ultrasonic waves were supplied at 15–30 Hz for a time duration of 20 min for each fuel blend. The techniques used enabled the proper blending of nanoparticles in test fuel. Table 4 demonstrates the properties of test fuels.

Table 4. Physicochemical properties of test fuels.

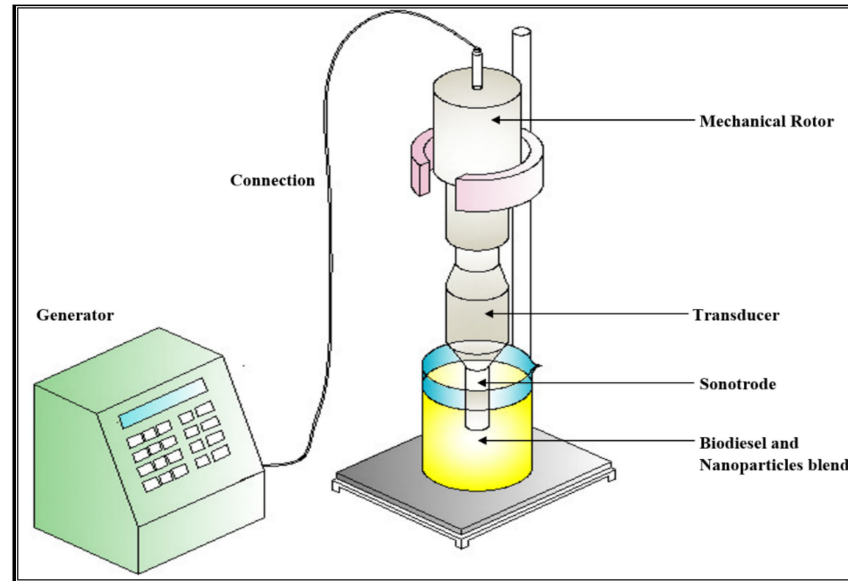| Properties	Unit	ASTM Test Standards	Diesel	SBME25	SBME25Ce-ZnO25	SBME25Ce-ZnO50	SBME25Ce-ZnO75
Density at 15 °C	kg/m^3	D4052	810	845.66	840.2	844.6	845.8
Calorific value	MJ/kg	D4868	45	41.684	43.10	44.35	44.15
Kinematic Viscosity at 40 °C	mm^2/s	D445	2.12	3.56	3.4	3.5	3.6
Cetane number	-	D613	51	48.66	51.6	52.8	52.9
Flash point	°C	D93	55	65.71	60.5	58.2	59
Pour point	°C	D97	−4	−6	−5.1	−5.8	−5.8

Figure 5. Schematic representation of probe sonicator.

3. Results and Discussion

In this section, the performance characteristics, such as BTE and BSFC; emission characteristics such as HC, NOx, smoke, and CO; and combustion characteristics, such as HRR and ID are evaluated for nano fuel blends at constant speed of 1500 rpm, IT of 23.5°BTDC, IP of 220 bar, and CR of 19.5. Figure 6 illustrates stepwise analysis of synthesized Ce-ZnO nanoadditives on the engine characteristics of VCR engine.
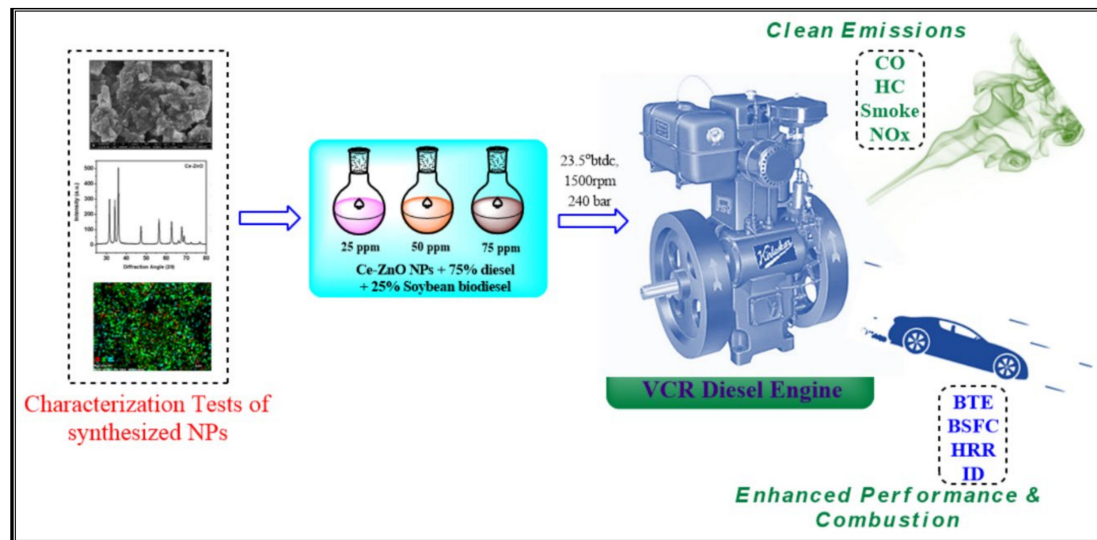

Figure 6. The analysis of synthesized Ce-ZnO nanoadditives on the engine characteristics of VCR engine.

3.1. Characterization of Nanoparticle

XRD technique was employed to analyze the purity and phase identification of the 3% Ce-ZnO nanostructures. Figure 7a depicts the XRD spectra of as-synthesized Ce-ZnO. In the figure, the strong (hkl) peaks at 2θ values of 31.59, 34.35, 35.99, 47.68, 56.81, and 61.24 are, respectively, equivalent to the lattice planes (100), (002), (101), (102), (110), and (103). The spectral data are in accordance with the JCPDS card No. 036-1451 and indicates that products are in the pure hexagonal ZnO phase of wurtzite [42,43]. The appearance of no cerium-related peak suggests that the cerium goes into ZnO lattice, and there is no change in the ZnO crystal structure upon doping. Debye–Scherer formula calculated the average size of 3% Ce-ZnO in crystallite. The average crystallite size of 3% Ce-ZnO nanostructures was found to be 12.16 nm. This decrease in 3% Ce-ZnO crystallite size is primarily due to the development of Ce–O–Zn on the sample's surface, which might, to some degree, impede the growth of ZnO nanoparticles. The room temperature optical absorption spectra of 3% Ce-ZnO is shown in Figure 7b. The absorption of lattices can provide details on the atomic vibrations involved. ZnO optical absorption edge typically was measured at 360 nm. The ZnO absorption edge clearly shifts with cerium doping (440 nm) towards the blue shift. Three-percent Ce-ZnO surface morphology was studied using FESEM. Figure 7c displays an as-synthesized sample FESEM image, which confirms the formation of 3% Ce-ZnO nanostructures. Figure 7c shows a large number of irregular counter-like nanostructures ranging 50–80 nm in size. The elemental composition of 3% Ce-ZnO (Figure 7d) was confirmed by energy dispersive spectroscopy (EDS). For the 3% Ce-ZnO, the chemical composition of Ce, Zn, and O atomic ratios was found to be 2.58, 58.90, and 38.52, respectively. The non-existence of peaks in relation to any other impurity element indicates that only Ce, Zn, and O are composed of the synthesized material.
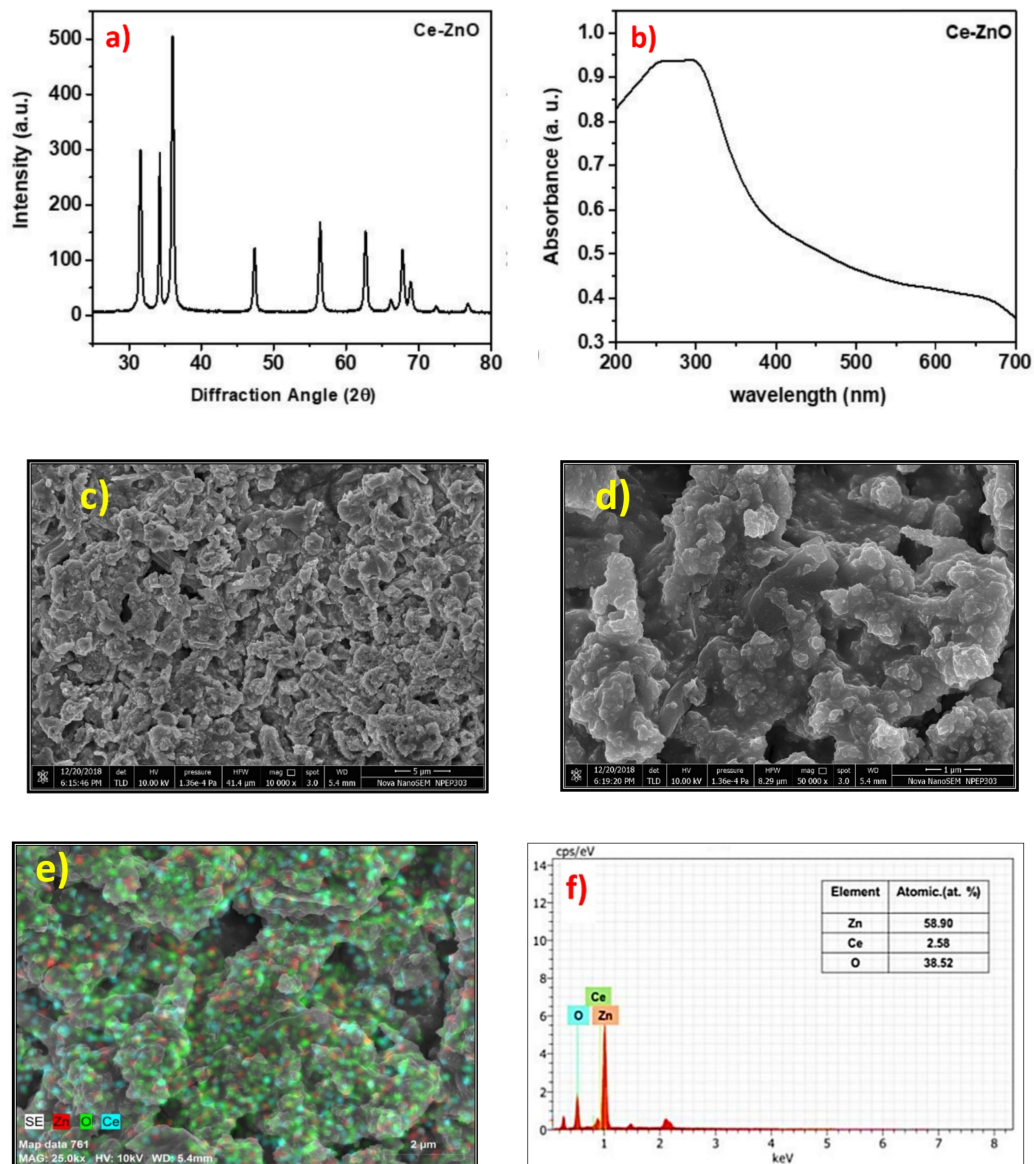
Figure 7. The characterization using: (**a**) XRD; (**b**) UV-vis; (**c**) FESEM (10000× magnification); (**d**) FESEM (50000× magnification); (**e**) EDS and (**f**) EDS histogram.

Microexplosion is caused by heterogeneous nucleation, where nucleation occurs at the droplet surface. Once the nanoparticles encased in water droplet biodiesel emulsion are exposed to high pressure and temperature environment in the engine cylinder, the water droplets will absorb the heat rapidly due to the lower boiling point of water in comparison to the biodiesel. This effect results in the explosion of water droplets through the surrounding oil layers known as microexplosion. Accordingly, secondary fuel droplets of very fine size are formed, which in turn evaporate quickly. Therefore, the formation of secondary droplets in the combustion chamber enhances the fuel–air mixing in the presence of potential NPs. Fuel blends with nanoadditives lead to enhanced microexplosion phenomenon, which results in reduction in the level of toxic pollutants in the exhaust gases and improvement in combustion rate with comparison with the biodiesel without additives [35,44]. Figure 8 shows the microexplosion phenomenon.
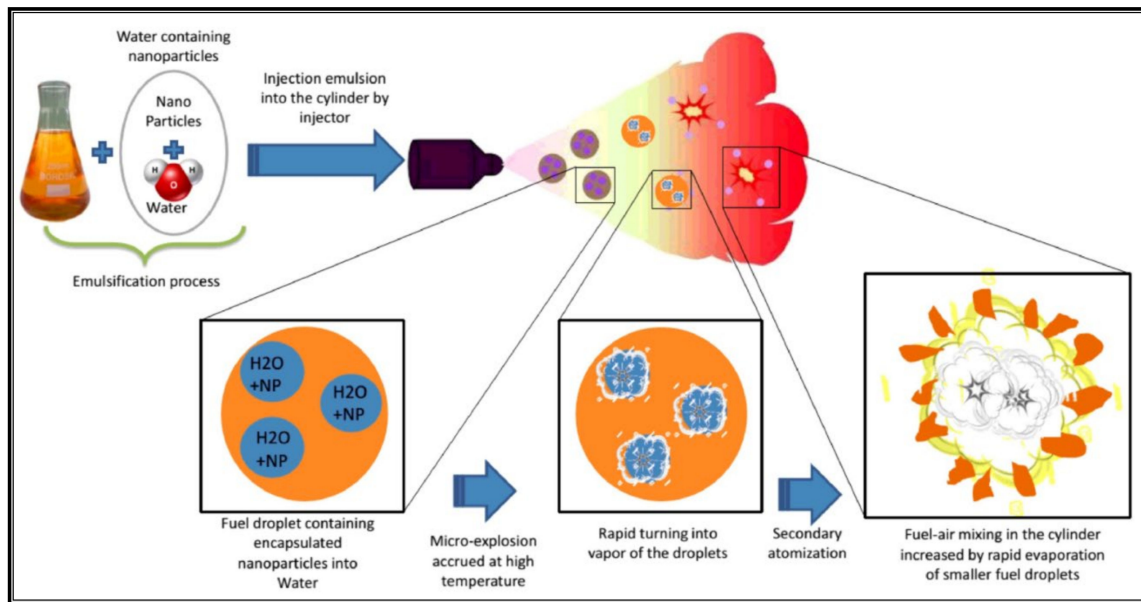
Figure 8. Microexplosion phenomenon [45] (Adapted with permission from Elsevier B.V., Progress in Energy and Combustion Science., License Number: 4893860601611).
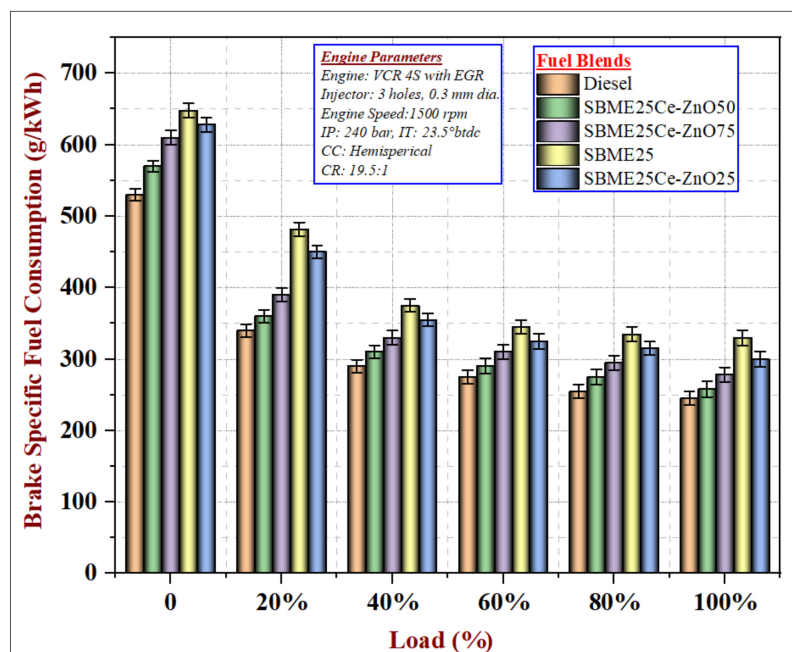
3.2. The Influence of Fuel Blends on Performance Characteristics

Figure 9a shows the variation of BTE with load for different test fuels, and the VCR engine was run at a constant speed and a CR of 19.5. A surge in BTE was observed with the rising loads; the highest BTE value was observed for a load of 80% [22,41]. The properties of the SBME25 fuel blend indicated lower calorific value and inferior cold flow properties. The engine operation showed lower BTE value for SBME25 fuel blend at all loads. At full load, the BTE for SBME25, SBME25Ce-ZnO25, SBME25Ce-ZnO50, and SBME25Ce-ZnO75 were 24.2%, 25.9%, 29.2%, and 27%, respectively. The findings reveal that the addition of Ce-ZnO nanoparticles in the Soybean biodiesel increases the BTE at all loads. The Ce-ZnO nanoparticles in the fuel blends encourage the microexplosion phenomenon, which results in comprehensive combustion of fuel particles [46,47]. The fuel blend SBME25Ce-ZnO50 demonstrated the highest BTE value, and the BTE increased by 20.66% and 11.5% for 75 ppm of Ce-ZnO when compared to SBME25. A previous study by Mujtaba et al. [8] showed an increase in BTE by on average 8.01% and 5.49% for dimethyl carbonate (DMC) and titanium dioxide (TiO_2) additive with B30 blend, respectively, compared to b30 blends without additives at full load operation. Thus, addition of nanoparticle was found to be improve the BTE.

Figure 9b demonstrates BSFC with load variation for different fuel blends. The BSFC is the ratio of the rate of fuel consumed and the amount of BP generated. The loads were varied, and the readings were drawn at maximum load. The SBME25 fuel blend illustrated the highest BSFC due to lower calorific value and poor cold flow properties, which results in incomplete fuel combustion. The BSFC for the blends with the Ce-ZnO nanoparticles illustrated lower emissions owing to higher O_2, which assists incomplete fuel combustion and enhances the microexplosion phenomenon [22,33]. The fuel blends SBME25Ce-ZnO25, SBME25Ce-ZnO50, and SBME25Ce-ZnO75 reduced the BSFC by 9.1%, 21.81%, and 15.75%, respectively, compared to SBME25. The higher CR of 19.5 and higher surface to area ratio of Ce-ZnO nanoparticles aided in thorough combustion of fuel. Previous study by Mujtaba et al. [8] showed an a reduction in BSFC reduction by 6.76% and 1.45% for B30 + TiO_2 and B30 + DMC blends in comparison with unblended B30. Thus, addition of nanoparticle was found to improve the BSFC.
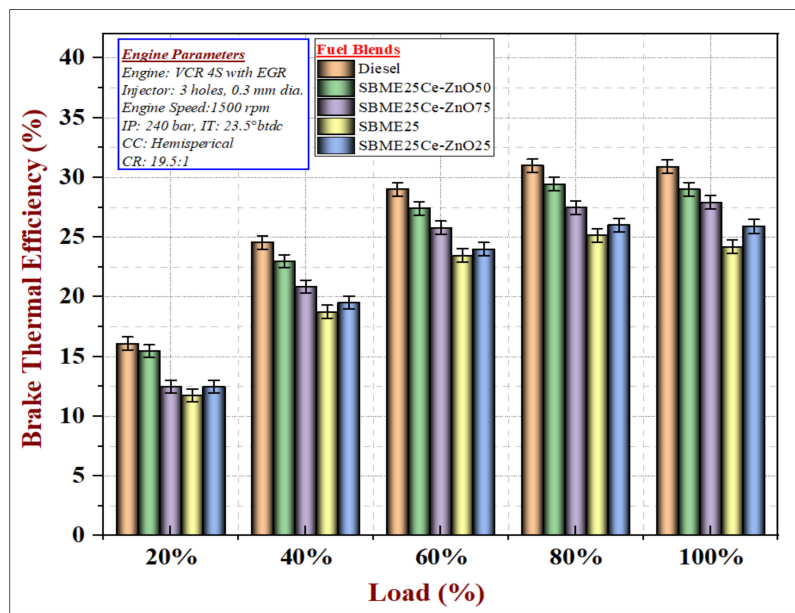
(**a**)

(**b**)

Figure 9. Variation with load for different fuel blends of: (**a**) BTE; and (**b**) BSFC.

3.3. The Influence of Fuel Blends on Engine Emission Characteristics

3.3.1. CO Emission

CO is primarily generated because of the improper combustion of carbon in the H-C chain. According to the United States Environmental Protection Agency (EPA), about 95% of all CO emissions are emitted from motor vehicle exhaust [48]. Figure 10 sows the variation of CO with load for different fuel blends. The Ce-ZnO nanoparticles encourage thorough combustion of the fuel particles in comparison with the neat biodiesel fuel blends. Hence, the blends with Ce-ZnO nanoparticles illustrated the lowest CO emissions as a result of complete fuel combustion amongst all the fuels caused

by the existence of fuel borne O_2 molecules and surface reactive area (Ce-ZnO), which lead to high mean combustion chamber temperature and also high pressure due to CR 19.5. The CO emissions for SBME25, SBME25Ce-ZnO25, SBME25Ce-ZnO50, and SBME25Ce-ZnO75 are 0.3, 0.28, 0.21, and 0.25% vol. respectively. The emissions reduced by 6.6%, 30%, and 16.5% for concentrations of 25, 50, and 75 ppm, respectively, for the Ce-ZnO nanoparticles in biodiesel compared to soybean biodiesel. Örs et al. [49] found that addition of TiO_2 in B20 resulted in 10.83% and 25.56% CO reduction compared to B20 and petroleum diesel, respectively. A similar observation was reported by Saxena et al. [50].
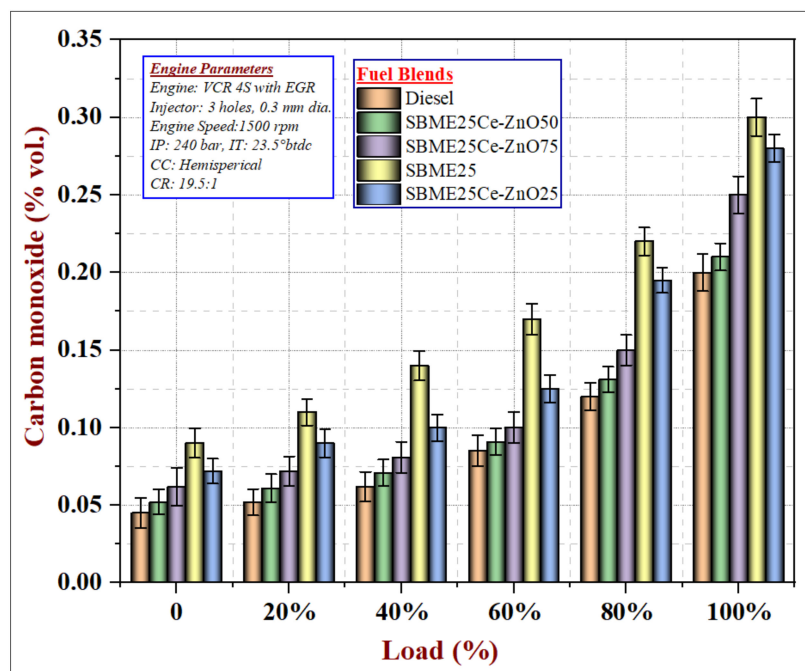

Figure 10. Variation of CO with load for different fuel blends.

3.3.2. NOx Emission

NOx is generated from the reaction between two gases, viz. N_2 and O_2, during the combustion process, usually at high temperatures [51]. The nitrogen oxide emissions for the catalysts are generally higher than the neat fuel blends. Figure 11 illustrates the variation of NOx and load for various fuel blends. At full load, the emissions of NOx produced for the nano fuel blends SBME25Ce-ZnO25, SBME25Ce-ZnO50, and SBME25Ce-ZnO75 are 490.8, 525.15, and 588.71 ppm, respectively. The rise in the concentrations of Ce-ZnO nanoparticles in SBME25 fuel blends increases the NOx due to the increase in the combustion chamber temperature and excess oxygen atoms due to oxygen donating nanoparticles. The NOx rises by 11.46% for 25 ppm of Ce-ZnO in the SBME25 fuel blend compared to SBME25.

3.3.3. Smoke Emission

Residual carbon atoms in exhaust gas are known as soot or smoke opacity. Fuel atomization and lack of oxygen are the two key elements that affect smoke emissions in CI engines [52,53]. In Figure 12, the smoke opacity rises with a rise in the engine loading conditions due to the rich A:F mixture in the combustion chamber. The neat soybean biodiesel (SBME25) presents higher smoke due to incomplete fuel combustion at all loading conditions. Adding Ce-ZnO nanoparticles in the test fuel reduced the smoke considerably. The smoke opacity for fuel blend SBME25Ce-ZnO50 was similar to D100 at all loads. The addition of a higher dosage level of Ce-ZnO nanoparticles slightly increases the smoke emissions due to rich air and fuel ratio. The smoke opacity for fuel blends SBME25Ce-ZnO25, SBME25Ce-ZnO50, and SBME25Ce-ZnO75 at maximum load are 55.71, 49.2 and 51.4 HSU, and the

reduction in smoke was 8.2%, 18.7%, and 15.3% when contrasted with the soybean biodiesel (B25) fuel blend, respectively. This is caused by an enhancement in the microexplosion phenomenon, which enables complete fuel combustion.
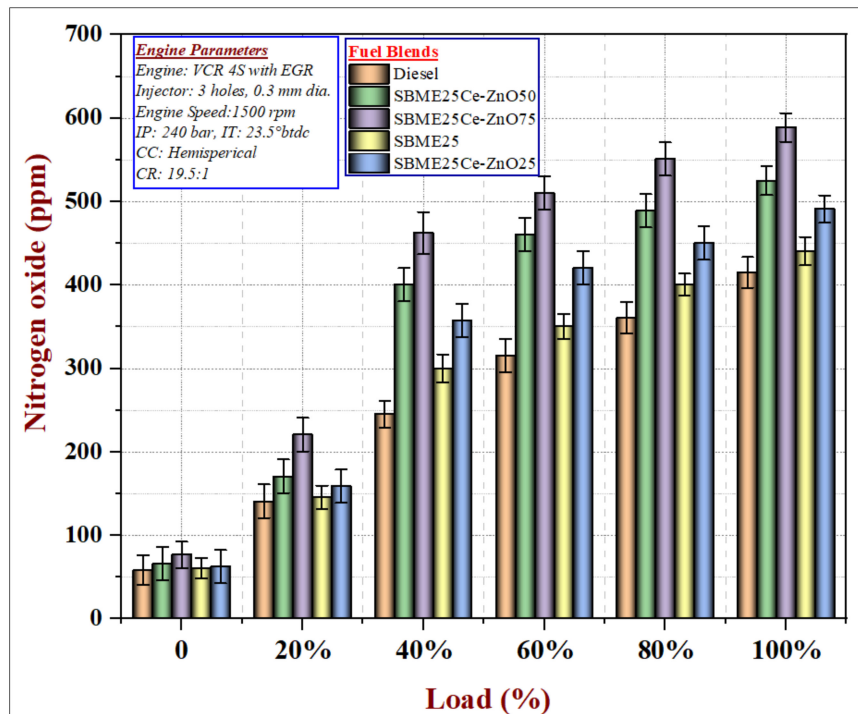
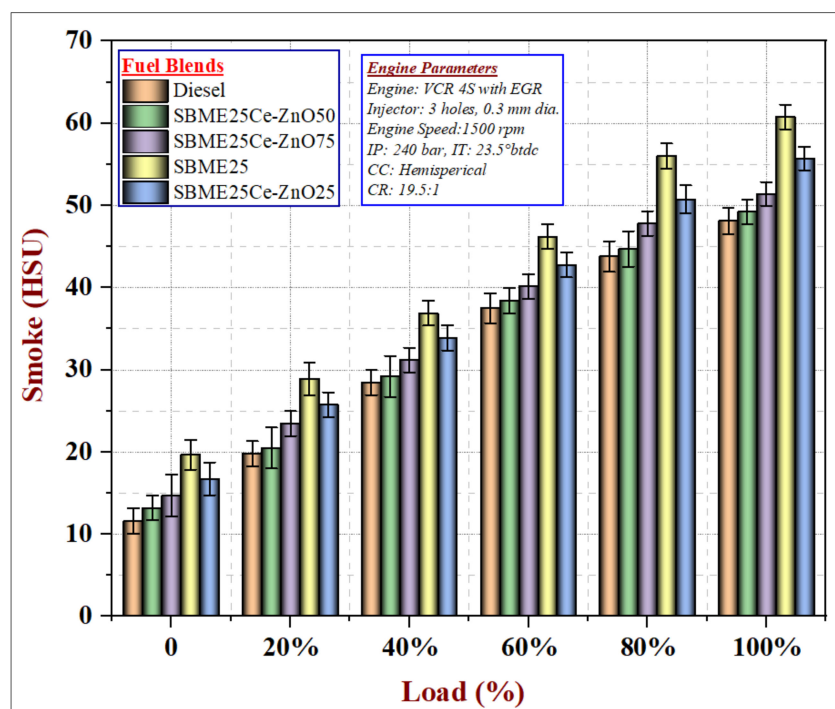**Figure 11.** Variation of NOx with load for different fuel blends.

Figure 12. Variation of smoke with load for different fuel blends.

3.3.4. Hydrocarbon Emission

Figure 13 describes HC emissions vs. load variation for neat SBME25 and nano fuel blends. HC emissions are comprised of unburned particles of fuel because of the lower temperature close to the cylinder wall [53]. The HC emissions can be lowered by facilitating appropriate residence time for the oxidation phenomenon, increasing the combustion chamber (CC) temperature, and combining the HC with oxidizing gases. The presence of nanoparticles in the biodiesel blends lowers the HC owing to higher CC temperature. The neat SBME25 fuel blends increase the HC emissions due to the cooling effect, while, due to rapid and effective combustion provided by the Ce-ZnO nanoparticles, the HC emissions reduce. The HC emissions for the fuel blends SBME25Ce-ZnO25, SBME25Ce-ZnO50, and SBME25Ce-ZnO75 are reduced by 10%, 21.5%, and 19.1%, respectively, compared to SBME25 fuel blend.
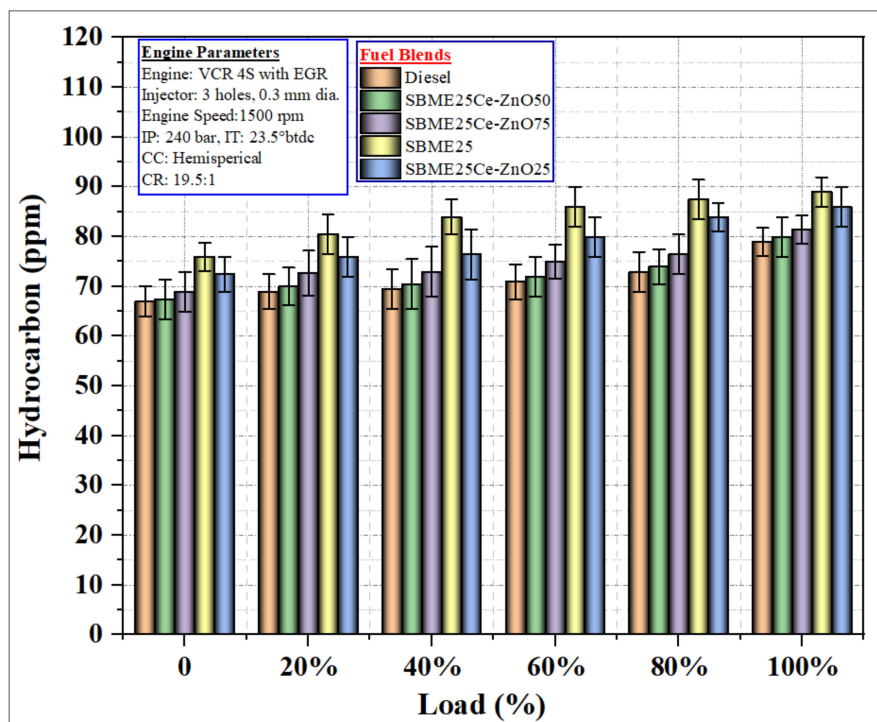

Figure 13. Variation of HC with load for different fuel blends.

3.4. Influence on Engine Combustion Characteristics

3.4.1. Heat Release Rate

The critical parameters influencing of HRR are the energy content, cetane number (CN), and viscosity of the fuel [54]. The combustion phenomenon begins early because of the enhanced ignition characteristics of Ce-ZnO nanoparticles in the SBME25 fuel blends. Figure 14 shows the behavior of HRR at different crank angles.

The HRR is calculated by applying the 1st law-single zone model shown in the Equation (1),

$$\frac{dQ_n}{d\theta} = \frac{\gamma_h}{\gamma_h - 1} \times p\frac{dV}{d\theta} + \frac{1}{\gamma_h - 1} \times V\frac{dp}{d\theta} + \frac{dQ_w}{d\theta} \qquad (1)$$

where $\frac{dQ_n}{d\theta}$ is the heat release rate, "T_m" is the mean in-cylinder temperature, $\left(\frac{dQ_w}{d\theta}\right)$ is the heat transfer rate from the gases to the cylinder wall, P is the cylinder pressure, and V is the volume of combustion chamber.
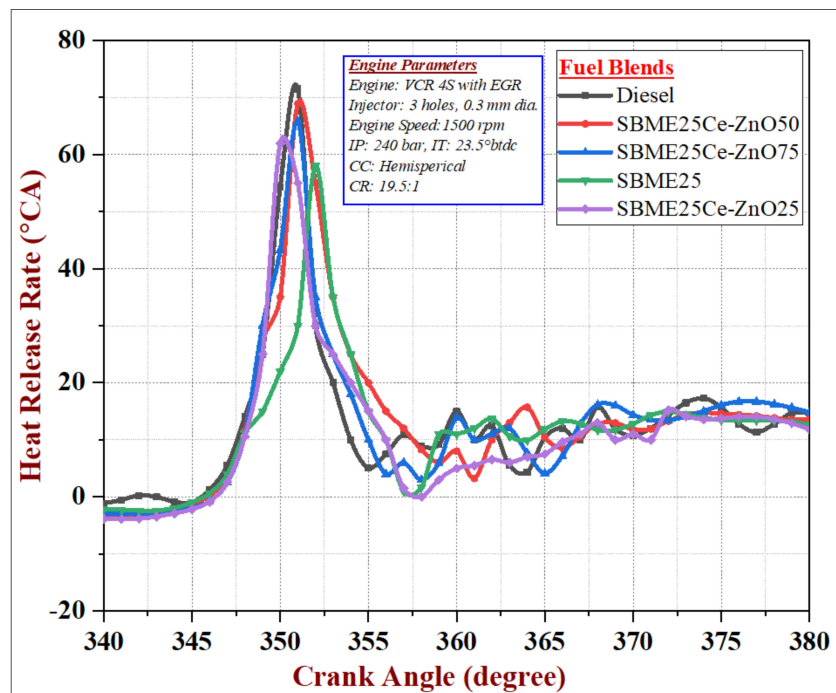
Figure 14. Variation of HRR at different crank angles.

The specific heat γ_h is illustrated in Equation (2),

$$\gamma_h = 1.35 - 6 \times 10^{-5} \times Tm + 10^{-8} \times T_m{}^2 \qquad (2)$$

The HRR for SBME25 fuel is lower in comparison with nano fuel blends as a result of higher molecular weight and lower burning velocity. In addition, CR 19.5 facilitates an improvement in the HRR as a result of higher pressure and combustion rate resulting in complete fuel combustion leading to elevated energy yield. The peak HRR values observed for the fuel blends SBME25Ce-ZnO25, SBME25Ce-ZnO50, and SBME25Ce-ZnO75 are 62.1, 68.5, and 65.7 °CA, respectively. The HRR increases by 7.06%, 18.1%, and 13.2% for Ce-ZnO nanoparticles concentration of 25, 50, and 75 ppm in comparison with the neat SBME25. The Ce-ZnO nanoparticles in the SBME25 fuel assist in better fuel atomization and supply higher oxygen content for complete fuel combustion [55,56].

3.4.2. Ignition Delay

ID period depends on the fuel type and their percentage in the CC. The factors accountable for regulating the length of the ID period of a diesel engine are the temperature of the charge throughout compression stoke, energy release during the phase of pre-ignition, and heat transfer or heat loss to the surroundings. This delay period consists of the physical delay, wherein atomization, vaporization, and mixing of air fuel occur, and chemical delay attributed to pre-combustion reactions. The ID is higher at lower loadings conditions and rises gradually at elevated loads due to enhanced compression and adequate A:F mixture. Figure 15 illustrates the variation of HRR at different crank angles. At full load, the ID values for the fuel blends SBME25Ce-ZnO25, SBME25Ce-ZnO50, and SBME25Ce-ZnO75 are 9.15, 8.5 and 8.7°CA, and the reductions compared to the fuel blend SBME25 are 5.1%, 11.20% and 9.12%, respectively.
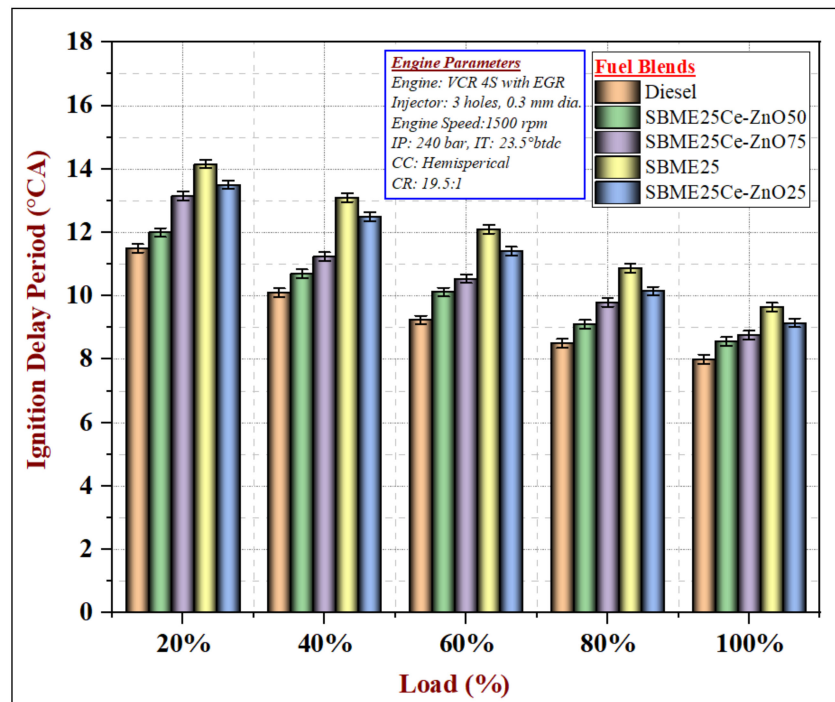
Figure 15. Variation of ID at different crank angles.

4. Conclusions

This paper reports the effect of different dosage Ce-ZnO nanoparticles (25, 50, and 75 ppm) and SBME25–diesel–span80 surfactant fuel blends on VCR CI engine characteristics at a CR 19.5, IT 23° BTDC, 1500 rpm, and varying loads. The diesel data are presented as reference only. The subsequent conclusions are derived based on the results achieved.

1. The physicochemical properties, for instance the calorific value and CN increase, and cold flow properties were enhanced by including Ce-ZnO nanoparticles in SBME25 fuel. In addition, the viscosity and density of all the nano fuel blend slightly reduced due to the addition of a 2% span80 surfactant compared to SBME25.
2. The laboratory synthesis of Ce-coated ZnO nanoparticles and soybean biodiesel considerably reduced the procurement cost of commercially available biodiesel and nanoparticles.
3. The ultrasonication process and addition of span80 enabled steady dispersal of Ce-ZnO nanoparticles in the biodiesel fuel blends.
4. The fuel blend SBME25Ce-ZnO50 illustrated a comprehensive enhancement in engine characteristics. At CR 19.5, Ce-ZnO nanoparticles in SBME25 enhanced the performance characteristics; 50 ppm of Ce-ZnO in SBME25 improved BTE by 20.6% and lowered the specific fuel consumption by 21.8% in comparison with SBME25 fuel blend.
5. The ternary fuel blends illustrated lower emissions; for SBME25Ce-ZnO50, the CO, HC, and smoke reduced by 30%, 21.5%, and 18.7% compared to SBME25 fuel blends, respectively, because of improved microexplosion and oxygen content, resulting in complete fuel combustion.
6. The combustion characteristics improved with the addition of Ce-ZnO in the SBME25 fuel blend: the HRR enhanced by 18.1% and the ID reduced by 11.2%.
7. SBME25Ce-ZnO50 showed best results for most criteria compared to other blends as well as SBME25 fuel operation.
8. The combustion, performance, and emission characteristics of SBME25Ce-ZnO50 operation were slightly worse than those of diesel operation.

The findings confirm that the Ce-ZnO nanoparticles in SBME25 at CR 19.5 improve the overall engine characteristics of the VCR engine compared to SBME25 operation.

Nomenclature

NPs	Nanoparticles	ZnO	Zinc oxide
VCR	Variable compression ratio	Ce	Cerium
CI	Compression ignition	Span80	Sorbitan oleate
nm	Nanometer	IC	Internal combustion
g/kWh	Grams per kilowatt hour	ppm	Parts per million
CC	Combustion chamber	m	Meter
ATDC	After top dead center	HCC	Hemispherical combustion chamber
FFA	Free fatty acid	BTDC	Before top dead center
ASTM	American Society for Testing and Materials	CR	Compression ratio
ID	Injection delay	PP	Peak pressure
CO_2	Carbon dioxide	HC	Hydrocarbon
NO_X	Oxides of nitrogen	CO	Carbon monoxide
BTE	Brake thermal efficiency	PM	Particulate matter
IP	Injection pressure	BSFC	Brake specific fuel consumption
IT	Injection timing	T_w	Wall temperature
HRR	Heat release rate	°CA	Crank angle (degrees)
D100	100% diesel	SBME	Soybean methyl ester (Soybean biodiesel)
SBME25	25% Soybean methyl ester blended with diesel	SBME25 Ce-ZnO25	SBME25 and 25 ppm Ce-ZnO NPs
SBME25 Ce-ZnO50	SBME25 and 50 ppm Ce-ZnO NPs	SBME25 Ce-ZnO75	SBME25 and 75 ppm Ce-ZnO NPs

References

1. Ashrafur Rahman, S.M.; Rainey, T.J.; Ristovski, Z.D.; Dowell, A.; Islam, M.A.; Nabi, M.N.; Brown, R.J. Review on the Use of Essential Oils in Compression Ignition Engines. In *Methanol and the Alternate Fuel Economy*; Agarwal, A.K., Gautam, A., Sharma, N., Singh, A.P., Eds.; Springer Singapore: Singapore, 2019; pp. 157–182. [CrossRef]
2. Rahman, S.A.; Hossain, F.; Van, T.C.; Dowell, A.; Islam, M.; Rainey, T.J.; Ristovski, Z.D.; Brown, R. Comparative evaluation of the effect of sweet orange oil-diesel blend on performance and emissions of a multi-cylinder compression ignition engine. In *Proceedings of the 7th Bsme International Conference on Thermal Engineering*; AIP Publishing: New York, NY, USA, 2017; Volume 1851, p. 20007. [CrossRef]
3. Rahman, S.M.A.; Mahila, T.M.I.; Ahmad, A.; Nabi, M.N.; Jafari, M.; Dowell, A.; Islam, M.A.; Marchese, A.J.; Tryner, J.; Brooks, P.R.; et al. Effect of Oxygenated Functional Groups in Essential Oils on Diesel Engine Performance, Emissions, and Combustion Characteristics. *Energy Fuels* **2019**, *33*, 9828–9834. [CrossRef]

4. Soudagar, M.E.M.; Nik-Ghazali, N.-N.; Kalam, M.A.; Badruddin, I.; Banapurmath, N.; Akram, N. The effect of nano-additives in diesel-biodiesel fuel blends: A comprehensive review on stability, engine performance and emission characteristics. *Energy Convers. Manag.* **2018**, *178*, 146–177. [CrossRef]

5. Mahlia, T.M.I.; Syazmi, Z.A.H.S.; Mofijur, M.; Abas, A.E.P.; Bilad, M.R.; Ong, H.C.; Silitonga, A.S. Patent landscape review on biodiesel production: Technology updates. *Renew. Sustain. Energy Rev.* **2020**, *118*, 109526. [CrossRef]

6. Harari, P.; Banapurmath, N.; Yaliwal, V.; Khan, T.Y.; Soudagar, M.E.M. Experimental studies on performance and emission characteristics of reactivity controlled compression ignition (RCCI) engine operated with gasoline and Thevetia Peruviana biodiesel. *Renew. Energy* **2020**, *160*, 865–875. [CrossRef]

7. Soudagar, M.E.M.; Afzal, A.; Kareemullah, M. Waste coconut oil methyl ester with and without additives as an alternative fuel in diesel engine at two different injection pressures. *Energy Sources Part A Recovery Utilization Environ. Effects* **2020**, 1–19. [CrossRef]

8. Mujtaba, M.; Masjuki, H.; Kalam, M.; Ong, H.C.; Gul, M.; Farooq, M.; Soudagar, M.E.M.; Ahmed, W.; Harith, M.; Yusoff, M. Ultrasound-assisted process optimization and tribological characteristics of biodiesel from palm-sesame oil via response surface methodology and extreme learning machine-Cuckoo search. *Renew. Energy* **2020**, *158*, 202–214. [CrossRef]

9. Mujtaba, M.; Masjuki, H.H.; Kalam, M.; Noor, F.; Farooq, M.; Ong, H.C.; Gul, M.; Soudagar, M.E.M.; Bashir, S.; Fattah, I.M.R.; et al. Effect of Additivized Biodiesel Blends on Diesel Engine Performance, Emission, Tribological Characteristics, and Lubricant Tribology. *Energies* **2020**, *13*, 3375. [CrossRef]

10. Silitonga, A.; Masjuki, H.; Mahlia, T.; Ong, H.; Chong, W.; Boosroh, M. Overview properties of biodiesel diesel blends from edible and non-edible feedstock. *Renew. Sustain. Energy Rev.* **2013**, *22*, 346–360. [CrossRef]

11. Fattah, I.M.R.; Masjuki, H.H.; Kalam, M.A.; Hazrat, M.A.; Masum, B.M.; Imtenan, S.; Ashraful, A.M. Effect of antioxidants on oxidation stability of biodiesel derived from vegetable and animal based feedstocks. *Renew. Sustain. Energy Rev.* **2014**, *30*, 356–370. [CrossRef]

12. Ashraful, A.M.; Masjuki, H.H.; Kalam, M.A.; Rizwanul Fattah, I.M.; Imtenan, S.; Shahir, S.A.; Mobarak, H.M. Production and comparison of fuel properties, engine performance, and emission characteristics of biodiesel from various non-edible vegetable oils: A review. *Energy Convers. Manag.* **2014**, *80*, 202–228. [CrossRef]

13. Farade, R.A.; Abdul Wahab, N.I.; Mansour, D.-E.A.; Azis, N.B.; Soudagar, M.E.M.; Siddappa, V. Development of Graphene Oxide-Based Nonedible Cottonseed Nanofluids for Power Transformers. *Materials* **2020**, *13*, 2569. [CrossRef] [PubMed]

14. Silitonga, A.; Shamsuddin, A.; Mahlia, T.; Milano, J.; Kusumo, F.; Siswantoro, J.; Dharma, S.; Sebayang, A.; Masjuki, H.; Ong, H.C. Biodiesel synthesis from Ceiba pentandra oil by microwave irradiation-assisted transesterification: ELM modeling and optimization. *Renew. Energy* **2020**, *146*, 1278–1291. [CrossRef]

15. Ong, H.C.; Milano, J.; Silitonga, A.S.; Hassan, M.H.; Shamsuddin, A.H.; Wang, C.T.; Mahlia, T.M.I.; Siswantoro, J.; Kusumo, F.; Sutrisno, J. Biodiesel production from Calophyllum inophyllum-Ceiba pentandra oil mixture: Optimization and characterization. *J. Clean. Prod.* **2019**, *219*, 183–198. [CrossRef]

16. Fattah, I.M.R.; Masjuki, H.H.; Liaquat, A.M.; Ramli, R.; Kalam, M.A.; Riazuddin, V.N. Impact of various biodiesel fuels obtained from edible and non-edible oils on engine exhaust gas and noise emissions. *Renew. Sustain. Energy Rev.* **2013**, *18*, 552–567. [CrossRef]

17. Liaquat, A.M.; Masjuki, H.H.; Kalam, M.A.; Rizwanul Fattah, I.M. Impact of biodiesel blend on injector deposit formation. *Energy* **2014**, *72*, 813–823. [CrossRef]

18. Khan, H.; Soudagar, M.E.M.; Kumar, R.H.; Safaei, M.R.; Farooq, M.; Khidmatgar, A.; Banapurmath, N.R.; Farade, R.A.; Abbas, M.M.; Afzal, A. Effect of Nano-Graphene Oxide and n-Butanol Fuel Additives Blended with Diesel—Nigella sativa Biodiesel Fuel Emulsion on Diesel Engine Characteristics. *Symmetry* **2020**, *12*, 961. [CrossRef]

19. Imtenan, S.; Varman, M.; Masjuki, H.H.; Kalam, M.A.; Sajjad, H.; Arbab, M.I.; Fattah, I.M.R. Impact of low temperature combustion attaining strategies on diesel engine emissions for diesel and biodiesels: A review. *Energy Convers. Manag.* **2014**, *80*, 329–356. [CrossRef]

20. Imtenan, S.; Masjuki, H.H.; Varman, M.; Rizwanul Fattah, I.M. Evaluation of n-butanol as an oxygenated additive to improve combustion-emission-performance characteristics of a diesel engine fuelled with a diesel-calophyllum inophyllum biodiesel blend. *RSC Adv.* **2015**, *5*, 17160–17170. [CrossRef]

21. Farade, R.A.; Wahab, N.I.B.A.; Mansour, D.-E.A.; Azis, N.B.; Jasni, J.; Banapurmath, N.; Soudagar, M.E.M. Investigation of the dielectric and thermal properties of non-edible cottonseed oil by infusing h-BN nanoparticles. *IEEE Access* **2020**, *8*, 76204–76217. [CrossRef]

22. S Gavhane, R.; M Kate, A.; Pawar, A.; Safaei, M.R.; M Soudagar, M.E.; Mujtaba Abbas, M.; Muhammad Ali, H.; R Banapurmath, N.; Goodarzi, M.; Badruddin, I.A. Effect of Zinc Oxide Nano-Additives and Soybean Biodiesel at Varying Loads and Compression Ratios on VCR Diesel Engine Characteristics. *Symmetry* **2020**, *12*, 1042. [CrossRef]

23. Soudagar, M.E.M.; Nik-Ghazali, N.-N.; Akram, N.; Al-Rashid, M.A.; Badruddin, I.A.; Khan, H.; Kallannavar, V.; Shahpurkar, K.; Afzal, A.; Farade, R.; et al. The potential of nanoparticle additives in biodiesel: A fundamental outset. In *Proceedings of the Advances in Mechanical Design, Materials and Manufacture*; AIP Publishing LLC: New York, NY, USA, 2020; p. 030003. [CrossRef]

24. Mujtaba, M.; Kalam, M.; Masjuki, H.; Gul, M.; Soudagar, M.E.M.; Ong, H.C.; Ahmed, W.; Atabani, A.; Razzaq, L.; Yusoff, M. Comparative study of nanoparticles and alcoholic fuel additives-biodiesel-diesel blend for performance and emission improvements. *Fuel* **2020**, *279*, 118434. [CrossRef]

25. Heidari-Maleni, A.; Gundoshmian, T.M.; Karimi, B.; Jahanbakhshi, A.; Ghobadian, B. A novel fuel based on biocompatible nanoparticles and ethanol-biodiesel blends to improve diesel engines performance and reduce exhaust emissions. *Fuel* **2020**, *276*, 118079. [CrossRef]

26. El-Seesy, A.I.; Hassan, H.; Ibraheem, L.; He, Z.; Soudagar, M.E.M. Combustion, emission, and phase stability features of a diesel engine fueled by Jatropha/ethanol blends and n-butanol as co-solvent. *Int. J. Green Energy* **2020**, 1–12. [CrossRef]

27. Akram, N.; Sadri, R.; Kazi, S.; Zubir, M.N.M.; Ridha, M.; Ahmed, W.; Soudagar, M.E.M.; Arzpeyma, M. A comprehensive review on nanofluid operated solar flat plate collectors. *J. Therm. Anal. Calorim.* **2020**, *139*, 1309–1343. [CrossRef]

28. Akram, N.; Sadri, R.; Kazi, S.; Ahmed, S.; Zubir, M.; Ridha, M.; Soudagar, M.; Ahmed, W.; Arzpeyma, M.; Tong, G.B. An experimental investigation on the performance of a flat-plate solar collector using eco-friendly treated graphene nanoplatelets–water nanofluids. *J. Therm. Anal. Calorim.* **2019**, *138*, 609–621. [CrossRef]

29. Fangsuwannarak, K.; Triratanasirichai, K. Improvements of palm biodiesel properties by using nano-TiO2 additive, exhaust emission and engine performance. *Rom. Rev. Precis. Mech. Opt. Mechatron* **2013**, *43*, 111–118.

30. Jung, H.; Kittelson, D.B.; Zachariah, M.R. The influence of a cerium additive on ultrafine diesel particle emissions and kinetics of oxidation. *Combust. Flame* **2005**, *142*, 276–288. [CrossRef]

31. Kumar, S.; Dinesha, P.; Rosen, M.A. Effect of injection pressure on the combustion, performance and emission characteristics of a biodiesel engine with cerium oxide nanoparticle additive. *Energy* **2019**, *185*, 1163–1173. [CrossRef]

32. Sivakumar, M.; Shanmuga Sundaram, N.; Ramesh kumar, R.; Syed Thasthagir, M.H. Effect of aluminium oxide nanoparticles blended pongamia methyl ester on performance, combustion and emission characteristics of diesel engine. *Renew. Energy* **2018**, *116*, 518–526. [CrossRef]

33. Sajith, V.; Sobhan, C.; Peterson, G. Experimental investigations on the effects of cerium oxide nanoparticle fuel additives on biodiesel. *Adv. Mech. Eng.* **2010**, *2*, 581407. [CrossRef]

34. Alagumalai, A. Combustion characteristics of lemongrass (Cymbopogon flexuosus) oil in a partial premixed charge compression ignition engine. *Alex. Eng. J.* **2015**, *54*, 405–413. [CrossRef]

35. Basha, J.S.; Anand, R. Performance, emission and combustion characteristics of a diesel engine using Carbon Nanotubes blended Jatropha Methyl Ester Emulsions. *Alex. Eng. J.* **2014**, *53*, 259–273. [CrossRef]

36. Fattah, I.M.R.; Masjuki, H.H.; Kalam, M.A.; Wakil, M.A.; Ashraful, A.M.; Shahir, S.A. Experimental investigation of performance and regulated emissions of a diesel engine with Calophyllum inophyllum biodiesel blends accompanied by oxidation inhibitors. *Energy Convers. Manag.* **2014**, *83*, 232–240. [CrossRef]

37. Fattah, I.M.R.; Masjuki, H.H.; Kalam, M.A.; Mofijur, M.; Abedin, M.J. Effect of antioxidant on the performance and emission characteristics of a diesel engine fueled with palm biodiesel blends. *Energy Convers. Manag.* **2014**, *79*, 265–272. [CrossRef]

38. Fattah, I.M.R.; Masjuki, H.H.; Kalam, M.A.; Wakil, M.A.; Rashedul, H.K.; Abedin, M.J. Performance and emission characteristics of a CI engine fueled with Cocos nucifera and Jatropha curcas B20 blends accompanying antioxidants. *Ind. Crops Products* **2014**, *57*, 132–140. [CrossRef]

39. Moffat, R.J. Describing the uncertainties in experimental results. *Exp. Therm. Fluid Sci.* **1988**, *1*, 3–17. [CrossRef]

40. Soudagar, M.E.M.; Nik-Ghazali, N.-N.; Kalam, M.; Badruddin, I.A.; Banapurmath, N.; Ali, M.A.B.; Kamangar, S.; Cho, H.M.; Akram, N. An investigation on the influence of aluminium oxide nano-additive and honge oil methyl ester on engine performance, combustion and emission characteristics. *Renew. Energy* **2020**, *146*, 2291–2307. [CrossRef]

41. Soudagar, M.E.M.; Nik-Ghazali, N.-N.; Kalam, M.; Badruddin, I.A.; Banapurmath, N.; Khan, T.Y.; Bashir, M.N.; Akram, N.; Farade, R.; Afzal, A. The effects of graphene oxide nanoparticle additive stably dispersed in dairy scum oil biodiesel-diesel fuel blend on CI engine: Performance, emission and combustion characteristics. *Fuel* **2019**, *257*, 116015. [CrossRef]

42. Naveed Ul Haq, A.; Nadhman, A.; Ullah, I.; Mustafa, G.; Yasinzai, M.; Khan, I. Synthesis approaches of zinc oxide nanoparticles: The dilemma of ecotoxicity. *J. Nanomater.* **2017**, *2017*, 8510342. [CrossRef]

43. Hasnidawani, J.; Azlina, H.; Norita, H.; Bonnia, N.; Ratim, S.; Ali, E. Synthesis of ZnO nanostructures using sol-gel method. *Procedia Chem.* **2016**, *19*, 211–216. [CrossRef]

44. Sadhik Basha, J.; Anand, R. Role of nanoadditive blended biodiesel emulsion fuel on the working characteristics of a diesel engine. *J. Renew. Sustain. Energy* **2011**, *3*, 023106. [CrossRef]

45. Khalife, E.; Tabatabaei, M.; Demirbas, A.; Aghbashlo, M. Impacts of additives on performance and emission characteristics of diesel engines during steady state operation. *Prog. Energy Combust. Sci.* **2017**, *59*, 32–78. [CrossRef]

46. Annamalai, M.; Dhinesh, B.; Nanthagopal, K.; Sivarama Krishnan, P.; Lalvani, J.I.J.; Parthasarathy, M.; Annamalai, K. An assessment on performance, combustion and emission behavior of a diesel engine powered by ceria nanoparticle blended emulsified biofuel. *Energy Convers. Manag.* **2016**, *123*, 372–380. [CrossRef]

47. Ashok, B.; Nanthagopal, K.; Mohan, A.; Johny, A.; Tamilarasu, A. Comparative analysis on the effect of zinc oxide and ethanox as additives with biodiesel in CI engine. *Energy* **2017**, *140*, 352–364. [CrossRef]

48. EPA. *Latest Findings on National Air Quality: Status and Trends through 2006*; U.S. Environmental Protection Agency: Durham, NC, USA, 2008.

49. Örs, I.; Sarıkoç, S.; Atabani, A.E.; Ünalan, S.; Akansu, S.O. The effects on performance, combustion and emission characteristics of DICI engine fuelled with TiO2 nanoparticles addition in diesel/biodiesel/n-butanol blends. *Fuel* **2018**, *234*, 177–188. [CrossRef]

50. Saxena, V.; Kumar, N.; Saxena, V.K. Multi-objective optimization of modified nanofluid fuel blends at different TiO2 nanoparticle concentration in diesel engine: Experimental assessment and modeling. *Appl. Energy* **2019**, *248*, 330–353. [CrossRef]

51. Palash, S.M.; Kalam, M.A.; Masjuki, H.H.; Masum, B.M.; Rizwanul Fattah, I.M.; Mofijur, M. Impacts of biodiesel combustion on NOx emissions and their reduction approaches. *Renew. Sustain. Energy Rev.* **2013**, *23*, 473–490. [CrossRef]

52. Raju, V.D.; Kishore, P.; Nanthagopal, K.; Ashok, B. An experimental study on the effect of nanoparticles with novel tamarind seed methyl ester for diesel engine applications. *Energy Convers. Manag.* **2018**, *164*, 655–666. [CrossRef]

53. Venu, H.; Raju, V.D.; Subramani, L. Combined effect of influence of nano additives, combustion chamber geometry and injection timing in a DI diesel engine fuelled with ternary (diesel-biodiesel-ethanol) blends. *Energy* **2019**, *174*, 386–406. [CrossRef]

54. Fattah, I.M.R.; Ming, C.; Chan, Q.N.; Wehrfritz, A.; Pham, P.X.; Yang, W.; Kook, S.; Medwell, P.R.; Yeoh, G.H.; Hawkes, E.R.; et al. Spray and Combustion Investigation of Post Injections under Low-Temperature Combustion Conditions with Biodiesel. *Energy Fuels* **2018**, *32*, 8727–8742. [CrossRef]

55. Karthikeyan, S.; Elango, A.; Prathima, A. Performance and emission study on zinc oxide nano particles addition with pomolion stearin wax biodiesel of CI engine. *J. Sci. Ind. Res.* **2014**, *73*, 187–190.

56. Prabu, A. Nanoparticles as additive in biodiesel on the working characteristics of a DI diesel engine. *Ain Shams Eng. J.* **2018**, *9*, 2343–2349. [CrossRef]